Carbon Composite Foam for Multi Radionuclide Trap

Prasanta Jana[*1], V. Ganesan[2]

[1]Institute Jean Lamour (IJL-CNRS), ENSTIB, 27, Rue Philippe Séguin, 88026, Epinal, France

[2]Reactor Operations and Maintenance Group, Indira Gandhi Centre for Atomic Research Kalpakkam 603 102, India

[*1]pjanaigcar137@gmail.com; [2]ganesh@igcar.gov.in

***Abstract*-Carbon foam is employed for trapping fission products (^{137}Cs, ^{134}Cs) and nickel foam is employed for trapping activated corrosion products (^{54}Mn, ^{60}Co) from primary sodium system of fast reactor. However, deployment of individual radionuclide traps with associated shielding for each trap in the active building of a reactor demands larger floor space which has substantial financial implication. Hence, it is desirable to reduce the floor space requirement by incorporating multi radionuclide traps in single location. Therefore, it is necessary to search for materials (termed as multi-trap material) capable of trapping fission and activated corrosion product radionuclides of interest simultaneously from primary sodium circuit. In line with this, the present work describes the development of composite foam materials containing carbon and nickel for multi-trap application. This paper describes three different types of carbon composites namely nickel dispersed carbon foam (density 0.09 g. cm^{-3} and porosity 96%), nickel dispersed carbon coated alumina foam (density 0.03 g. cm^{-3} and porosity 99%) and carbon coated nickel foam (density 0.28 g. cm^{-3} and porosity 97%). The synthesis route of these carbon composite foams follow solution combustion route. By varying the reagents and quantities, the foam materials of interest were obtained. Such carbon composite foam materials are suitable for multi-trap applications.**

Keywords- Carbon Composite Foam; Multi Radionuclide Trap; Fission Products; Activated Corrosion Product; Activity Transport; Electron Microscopy

I. INTRODUCTION

An operating sodium cooled fast reactor, in addition to energy, produces radionuclides such as ^{54}Mn, ^{58}Co, ^{60}Co, ^{59}Fe, ^{51}Cr etc. in the core structural materials due to interaction of high neutron flux. They are released slowly into sodium coolant by diffusion and surface corrosion. In the event of fuel-clad failure, fission products such as ^{137}Cs, ^{134}Cs, ^{131}I, ^{140}Ba etc. are released into the coolant stream. These radionuclides are transported to various parts of primary heat transport system, get deposited and diffuse into the structural materials at out-of-core locations. The phenomenon of release, transport and deposition of radionuclides in the primary heat transport system is termed as activity transport. Due to activity transport, various issues are encountered which are listed below.

(a) High radiation shielding requirement for primary system components and pipelines;

(b) Restrictions of direct maintenance work;

(c) Radiological hazards resulting from any plausible primary sodium leak;

(d) Radiation burden during decontamination and disposal of primary components.

These issues, collectively, describe the quantum of radiation burden for operation and maintenance personnel in a fast reactor [1-3].

Release of fission product radionuclides in primary sodium could be minimized by removing the breached fuel immediately upon fission gas detection. But this conservative fuel management is not acceptable for commercial reactors from economic and plant operation point of view. For sodium coolant purification, cold trap is used universally. It works on the principle of reduction of solubility of impurity of interest with decreasing sodium temperature. The primary role of cold trap is to control the concentration of dissolved oxygen impurity in case of primary sodium system in addition to hydrogen and other elements of interest. The cold trap retains acceptable levels of activated corrosion products of structural materials and hence minimizes the release of such radionuclides to the primary system of fast reactor.

From the analysis of the cold trap data [1], it is observed that significant proportion of radioactive inventories can be removed from the coolant, but desired extent of removal of activated corrosion products viz. ^{54}Mn, ^{60}Co, ^{58}Co and fission products ^{137}Cs, ^{134}Cs is difficult. Therefore, special radionuclide trap to simultaneously trap multiple radionuclides is essential. The special radionuclide trap is a device located within the reactor primary sodium system that removes activated corrosion products or fission products (in the event of fuel pin failure) from coolant. The material present inside the special radionuclide trap device must retain the radionuclides of interest. Development of the special radionuclide trap device would also minimize the radiation burden during decontamination and disposal of primary components.

DOI: 10.5963/AMSA0303005

From literatures [4-10], it is known that most of the reactors preferred to employ carbon foam, namely, reticulated vitreous carbon (RVC) as getter material for trapping fission products ^{137}Cs and ^{134}Cs from primary sodium of fast reactor due to its open pore structure, high surface-to-volume ratio and very low density. Because of these properties, pressure drop across the trap employing RVC is lower than that of graphite granules for flow of liquid sodium through the trap, which is favourable for reactor operation. Indigenous carbon foam was developed to trap radioactive cesium from liquid sodium [11].

It is also reported in [12] that nickel foil with dimples to maintain interlayer spacing is preferred for use as ^{54}Mn trap in the form of modified fuel subassembly. It can also be seen from literature that nickel as foam material possesses unique features such as exceptional uniformity, lightweight, high porosity, intrinsic strength, corrosion resistance, and good electrical and thermal conductivities. If nickel foam is to be used for trapping activated corrosion products from primary sodium of fast reactor, several advantages can be visualized. As the porosity of nickel foam is 97.5%, the most important advantage of employing nickel foam as activated corrosion product trap would be low pressure drop of sodium flow compared to that of employing nickel foil as manganese trap in fuel subassembly. The authors have investigated the efficiency of nickel foam to trap Mn and Co from liquid sodium and compared the results with that using nickel foil. It was observed that nickel foam is more efficient than nickel foil [13, 14] in these studies.

As mentioned above, carbon foam can be employed for trapping fission products (^{137}Cs, ^{134}Cs) and nickel foam for trapping activated corrosion product (^{54}Mn, ^{60}Co) from primary sodium system of fast reactor. However, as stated at the beginning, deployment of individual radionuclide traps with associated shielding requirement calls for larger floor spacing in the active building of a reactor. The reactor active building, as a seismically qualified safety structure, any increase in floor space has an adverse effect on economics of building cost. Hence, it is desirable to reduce the floor space requirement by incorporating multi-radionuclide trap in single location. Therefore, it is necessary to search for the materials (termed as multi-trap material) capable of trapping fission and activated product radionuclides simultaneously from primary sodium. The present work describes the development of composite foam materials containing carbon and nickel for multi-trap application. The multi-trap is a novel concept being taken up currently and literature data on this topic are not available. The earlier work described carbon coated alumina foam for multi-trap application [15]. In this manuscript, synthesis and characterization of various carbon composites materials like Nickel Dispersed Carbon Foam (NDCF), Nickel Dispersed Carbon Coated Alumina Foam (NDCCAF) and Carbon Coated Nickel Foam (CCNF) are described elaborately.

II. EXPERIMENTAL

A. Synthesis

This paper describes three different types of carbon composites foams; NDCF, NDCCAF and CCNF. The synthesis routes of NDCF, NDCCAF and CCNF follow solution combustion route. For synthesizing NDCF, NDCCAF and CCNF, a common flowchart as shown in Fig. 1 is followed. By varying the reagents (A to E) and quantities as shown below in the steps (i)-(iii), the foam materials of interest were synthesized.

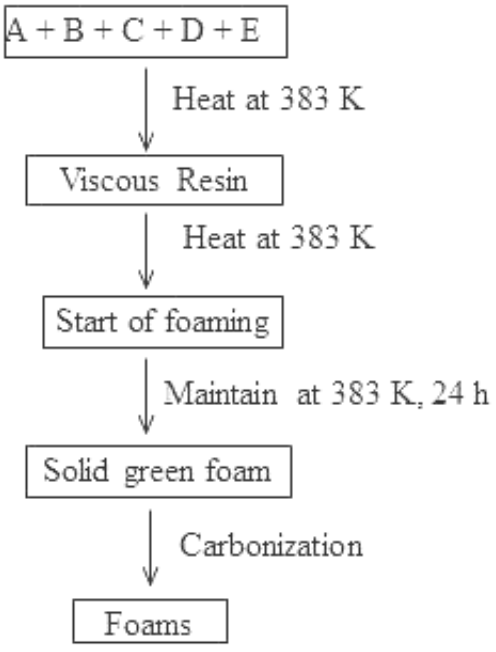

Fig. 1 Flowchart for preparation of foam materials

DOI: 10.5963/AMSA0303005

1) When A = sucrose (25 g), B = water (150 mL), C = $Ni(NO_3)_2.6H_2O$ (1 g), carbonization leads to the final product as NDCF.
2) When A = sucrose (25 g), B = water (150 mL), C = $Ni(NO_3)_2.6H_2O$ (0.5 g), D = $Al(NO_3)_3.9H_2O$ (8 g), carbonization leads to the final product as NDCCAF.
3) When A = sucrose (0.2 g), B = water (10 mL), E = nickel foam (0.1 g), carbonization leads to the final product as CCNF (no metal salts used).

Generally, there are two routes to synthesize foam materials, namely the template and the non-template methods. The template method is a technique using skeleton material of required shape and size, which is impregnated with required precursor followed by heat treatment to obtain replica of template material. In case of non-template method, the foam materials are synthesized directly from precursor without using template as a skeleton material. All the foam materials (NDCF and NDCCAF) mentioned above were synthesized without using template as skeleton. However, in the case of synthesis of CCNF, nickel foam was used as a template and sucrose as carbon source as described below.

1) NDCF

NDCF was synthesized from sucrose (99.5%, Sigma-Aldrich) and nickel nitrate hexahydrate (98.5%, Sigma-Aldrich). An aqueous solution containing 25 g of sucrose in 150 mL of distilled water with 1 g of $Ni(NO_3)_2.6H_2O$ was prepared in a Teflon beaker. The pH of this solution was found to be 0.8 (after solution preparation). The solution was slowly concentrated by heating at 383 K on a hot plate with constant stirring (100 rpm), till it turned into a dark viscous resin. After a while, the resin started foaming and continuous heating at 383 K in an air oven for a period of 24 h yielded dry foam. The green foam thus obtained was cut into regular shapes and carbonized in a furnace at a heating rate of 100 K. h^{-1} up to 1573 K in argon atmosphere with 2 h dwell time to obtain NDCF.

2) NDCCAF

NDCCAF was synthesized from nickel nitrate hexahydrate (98.5%, Sigma-Aldrich), aluminum nitrate nonahydrate (98%, Sigma-Aldrich) and sucrose (99.5%, Sigma-Aldrich). The synthesis route of NDCCAF is also comparable to NDCF; the only difference is in composition of the reactants. An aqueous solution containing 25 g of sucrose in 150 mL of distilled water with 8 g of $Al(NO_3)_3.9H_2O$ and 0.5 g of $Ni(NO_3)_2.6H_2O$ was prepared in a Teflon beaker. The pH of this solution was found to be 3.2 (after solution preparation). The green foam thus obtained was cut into regular shapes and carbonized in a furnace at a heating rate of 100 K. h^{-1} up to 1573 K in argon atmosphere with 2 h dwell time to obtain NDCCAF.

3) CCNF

An aqueous solution containing 0.2 g sucrose in 10 mL of distilled water was prepared in a Teflon beaker. Nickel foam (0.1 g) procured from M/s. Incofoam, Canada was immersed in this solution. The solution was heated at 383 K on a hot plate till the sucrose solution turned into a dry caramel. The caramel coated nickel foam sample was taken out from the beaker and heated to 1173 K in argon atmosphere with 2 h dwell time. Subsequent to heating, the sample was ultrasonically cleaned with distilled water and dried in oven.

B. Characterization

For characterization of green foam and carbonized foam materials, various characterizing tools were applied. For carrying out thermal analysis and X-ray diffraction, the green foam and carbonized foam were crushed using mortar and pestle to a fine powder and the respective spectra was recorded. The pore size of the foam samples was calculated from scanning electron microscopic images. Details of techniques used for characterization of foam samples are described below.

1) Thermal Analysis

As mentioned above, most of the green foams were prepared from sucrose-$Ni(NO_3)_2$ or sucrose-$Al(NO_3)_3$-$Ni(NO_3)_2$ and then carbonized in argon atmosphere. Therefore, thermal stability of most of the green foams was studied under argon atmosphere. The thermal stability of green foam was studied at a constant heating rate of 10 K. min^{-1} up to 1473 K. A high temperature thermo gravimetric analyzer (TGA, SETSYS 16/18 Evolution, Setaram, France) with a resolution of 1 μg was employed. For the purpose of evolved gas analysis, a quadrupole mass spectrometer (Pfeiffer Vacuum, Germany) was employed. The green foam sample in fine powder form was loaded in an alumina crucible, which was kept in the microbalance of TGA. Subsequently, the TGA system was evacuated and filled with argon gas. Evacuation and argon filling was done twice to minimize the residual oxygen and moisture levels in the furnace atmosphere. Argon was passed over the sample at a rate of 20 mL. min^{-1} throughout the experiment.

2) Phase Analysis

The room temperature X-ray diffractograms of NDCF and NDCCAF were recorded using X-ray diffractometer (Siemens D500, Germany) with Cu Kα radiation ($\lambda = 0.154056$ nm). The X-ray powder diffraction patterns were recorded in the angular range of 10–90 °with a step size of 0.05 °using monochromatic X-rays.

DOI: 10.5963/AMSA0303005

3) Surface Analysis

Surface morphology of the foams was examined by scanning electron microscope (SEM). The microstructures NDCF, NDCCAF and CCNF were obtained using SEM (Philips, XL30, The Netherlands). Pore size of the foams was calculated by using Image Pro Plus software. Inserting the SEM image in this software, micron bar (shown in SEM image also) is calibrated.

4) Elemental Analysis

Surface elemental compositions of NDCF, NDCCAF and CCNF were measured by energy dispersive X-ray (EDX) spectroscopy attached with the SEM. Elemental mapping was also performed on the foam samples to find out the distribution of elements over the foam surface.

5) Property Measurements

a) Density

Weight of the foam samples was measured using a microbalance. Since NDCF, NDCCAF, and CCNF could be shaped, their volumes were readily calculated by dimensional measurements and therefore, densities of foam materials were obtained by weight and volume ratio.

b) Porosity

The porosity of NDCF, NDCCAF, and CCNF was calculated using the following equation given below [16, 17]. Porosity = $100(1-\frac{\rho_b}{\rho_t})$. Where ρ_t is the theoretical density and ρ_b is the bulk density of the material.

III. RESULTS AND DISCUSSION

For the synthesis of all foam materials, sucrose was used, which played an important role to form porous network. Sucrose is a carbohydrate containing a six-member ring of glucose and a five-member ring of fructose. It is known that sucrose in acidic aqueous medium undergoes hydrolysis to form glucose and fructose as shown below.

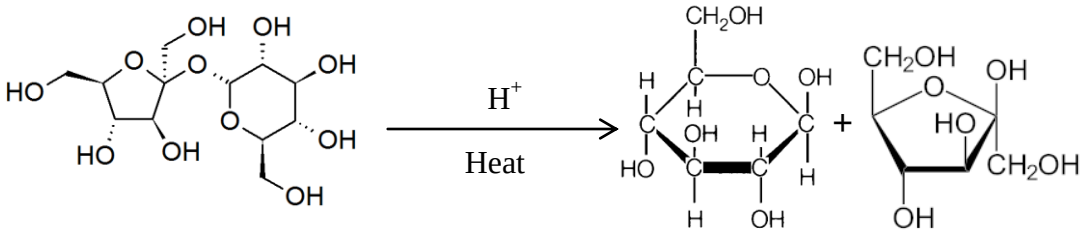

Sucrose Glucose Fructose

Acid (in the present case, nitric acid from nickel nitrate/aluminum nitrate) further oxidizes the glucose and fructose to a mixture of hydroxy carboxylic acids such as gluconic acid, saccharic acid, glycolic acid and tartaric acid [18]. Upon concentrating by heating, nitric acid-sucrose solution undergoes polymerization followed by condensation to form a resin. After several hours, the resin forms solid green foam [11].

A. NDCF

NDCF was synthesized using sucrose and $Ni(NO_3)_2$. Owing to the high degree of dissociation, $Ni(NO_3)_2$ in water is present mostly as constituent ions namely Ni^{2+}, NO^{3-}, H^+ and OH^-. Upon heating, the aqueous solution of sucrose-$Ni(NO_3)_2$ underwent polymerization and condensation to form a resin, which after a while formed a solid foam. The green foam thus formed was carbonized at 1573 K to obtain NDCF. The NDCF exhibited density of 0.09 g. cm^{-3} and porosity of 96%.

Thermal stability of NDCF (green foam) was studied in argon atmosphere. The mass loss of the green foam was noticed up to 775 K, thereafter no mass loss was observed. The green foam showed 73% mass loss in five stages (stage-I: 300-430 K, stage-II: 430-460 K, stage-III: 460-610 K, stage-IV: 610-680 K and stage-V: 680-775 K) as shown in Fig. 2. Stage-I was due to removal of H_2O from the green foam. In stage-II, gases corresponding to mass numbers 30, 44 and 46 were started evolving from the green foam as shown in Fig. 3. The gaseous decomposition products of mass numbers 2, 18, 28, 30, 44 and 46 were evolved from the green foam. From the evolved gas analysis, it was concluded that the gases which evolved from the green foam were H_2, H_2O, CO, NO, CO2 and NO_2. The base ion-current corresponding to mass number 32 (O_2) as shown in Fig. 3, indicates that O_2 as such is not evolved from the green foam. As the green foam was made of sucrose-$Ni(NO_3)_2$ and their reaction products, oxygen bearing species such as H_2O, CO, NO, CO_2 and NO_2 were evolved from the green foam during carbonization.

DOI: 10.5963/AMSA0303005

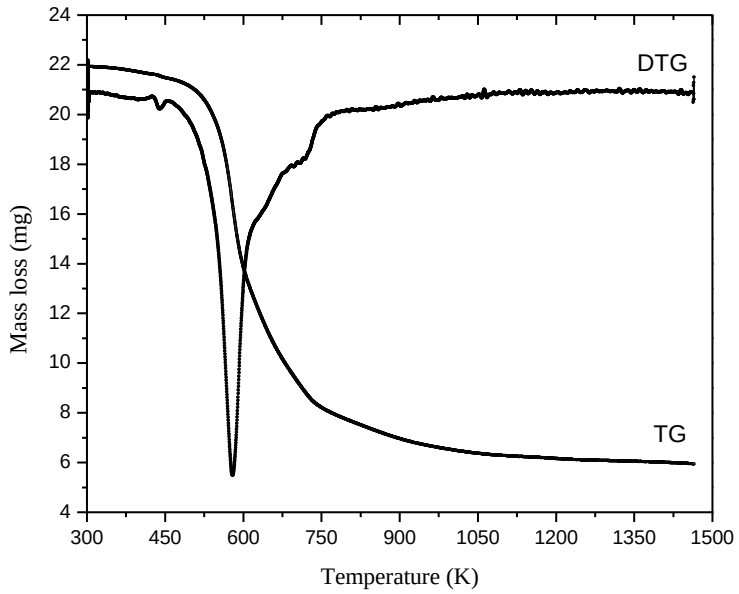

Fig. 2 Thermal decomposition pattern of NDCF (green foam)

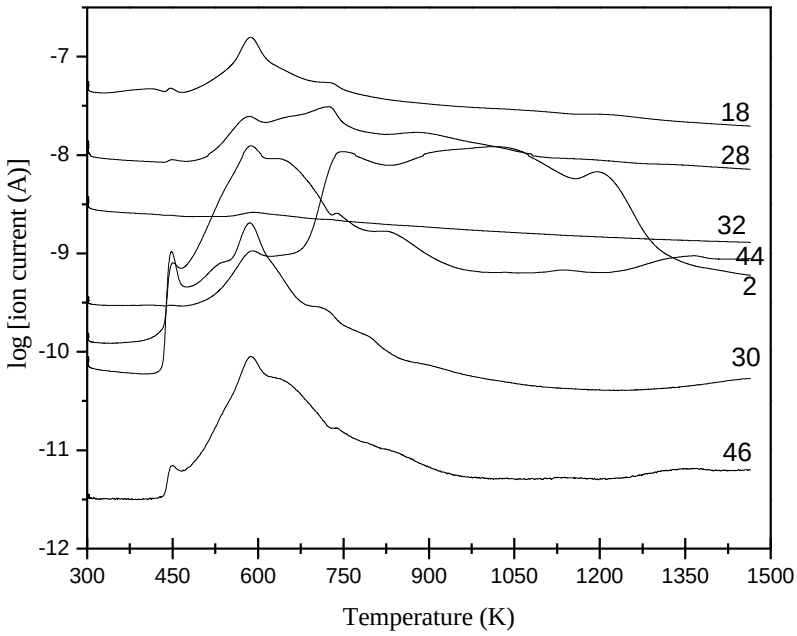

Fig. 3 Concentration of evolved gases from NDCF (green foam) as measured from respective ion currents as a function of temperature

Fig. 4 shows XRD pattern of green foam and NDCF carbonized at high temperature. The XRD pattern of green foam showed broad peak at 2θ value of 18.5 for carbon as shown in Fig. 4(a) and that was shifted to 26.1 due to slow graphitization of NDCF on carbonization at 1573 K as shown in Fig. 4(b). The NDCF carbonized at 1573 K showed peaks corresponding to carbon (JCPDS file no. 89-8487) and nickel (JCPDS file no. 04-0850). Generally, $Ni(OH)_2$ is decomposed at high temperature to form NiO. In the present case, NiO is reduced to nickel by CO and H_2 (evolved from the green foam during carbonization at high temperature). The possible mechanism of formation of nickel, which is dispersed on carbon foam matrix, is described below [19].

$$Ni(OH)_2 \rightarrow NiO + H_2O$$

$$NiO + CO \rightarrow Ni + CO_2$$

$$NiO + H_2 \rightarrow Ni + H_2O$$

DOI: 10.5963/AMSA0303005

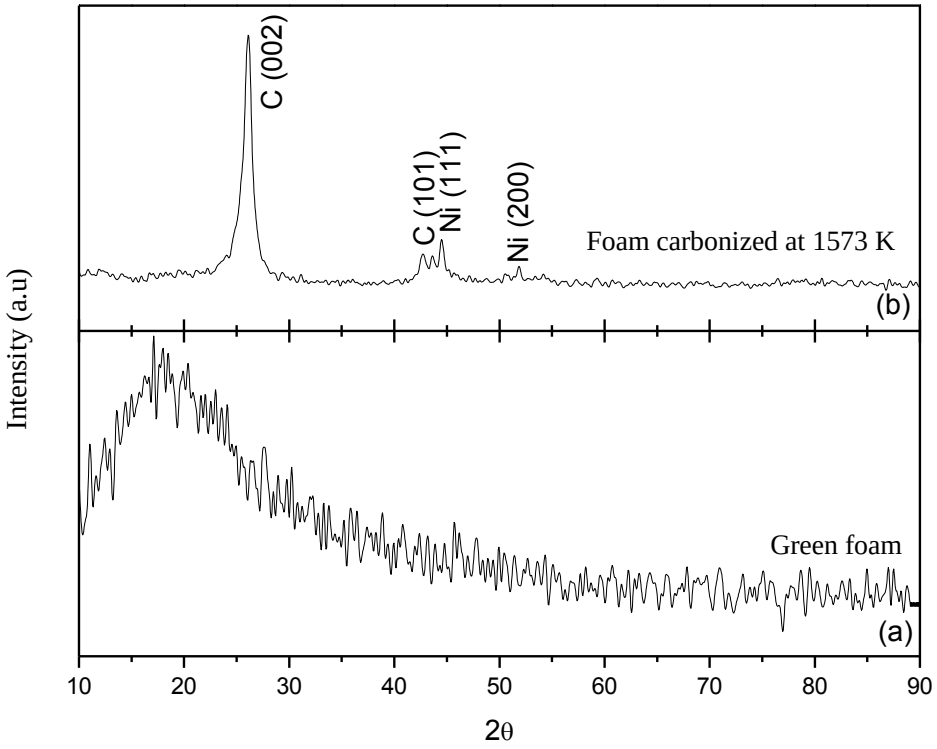

Fig. 4 XRD pattern of (a) NDCF (green foam) and (b) NDCF carbonized at 1573 K

Fig. 5(a) shows the secondary electron microscopic image of NDCF. It shows regular porous network of NDCF with 200 μm average pore size. To analyze the distribution of nickel over the foam surface, X-ray elemental mapping was carried out. Fig. 5(b) shows X-ray mapping of nickel showing uniform distribution over the foam surface (dimension of the foam 15 mm × 10 mm ×10 mm).

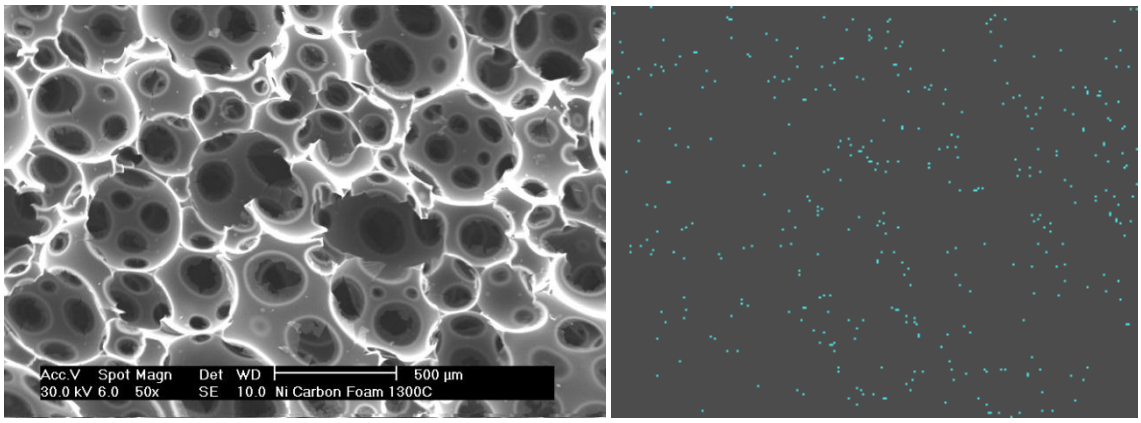

(a) (b)

Fig. 5 (a) Secondary electron microscopic image of NDCF and (b) X-ray mapping of nickel showing nickel distribution (color dots) over the foam surface

B. NDCCAF

NDCCAF was synthesized from $Ni(NO_3)_2$, $Al(NO_3)_3$ and sucrose. Here, all the reagents were base materials. Thermal stability of green foam was studied in argon atmosphere. The mass loss of the green foam was noticed up to 900 K after which no mass loss was observed as shown in Fig. 6. The green foam showed 65 wt% mass loss in four stages (stage-I: 300-435 K, stage-II: 435-530 K, stage-III: 530-635 K and stage-IV: 635-900 K). Stage-I was due to removal of H_2O from the green foam. Stages-II-IV correspond to decomposition of other volatile compounds present in the green foam. From the evolved gas analysis, it was concluded that the gases, which evolved from the green foam, were H_2, H_2O, NO, CO, CO_2 and NO_2 as shown in Fig. 7.

DOI: 10.5963/AMSA0303005

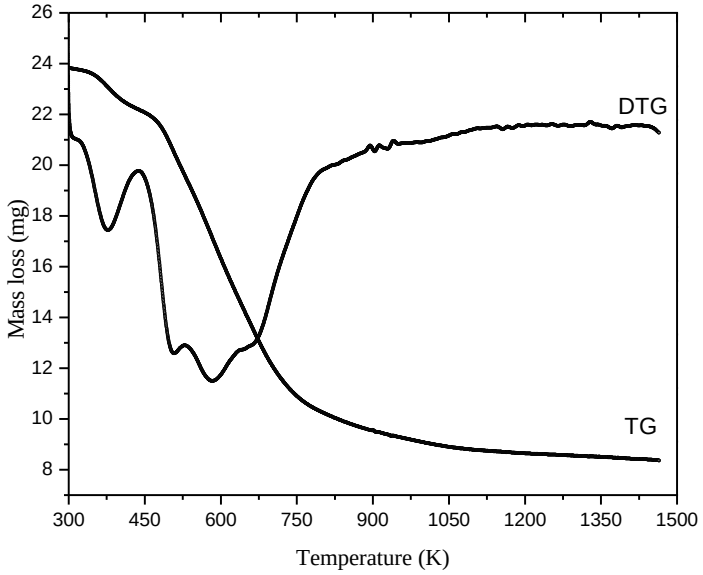

Fig. 6 Thermal decomposition pattern of NDCCAF (green foam)

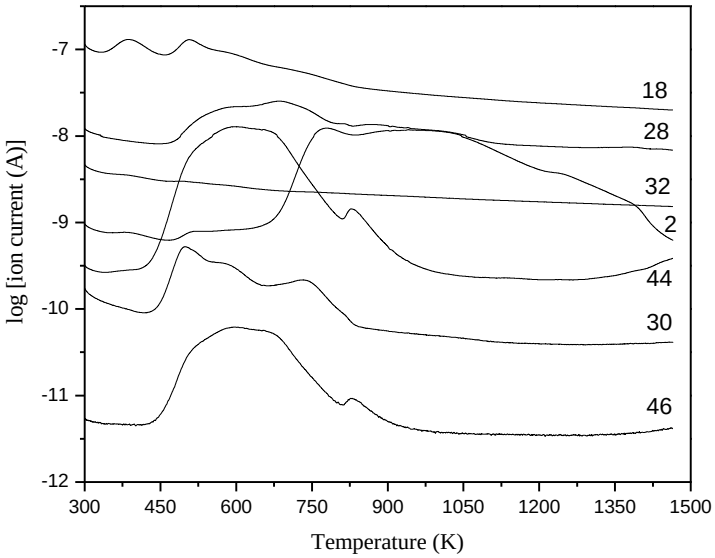

Fig. 7 Concentration of evolved gases from NDCCAF (green foam) as measured from respective ion currents as a function of temperature

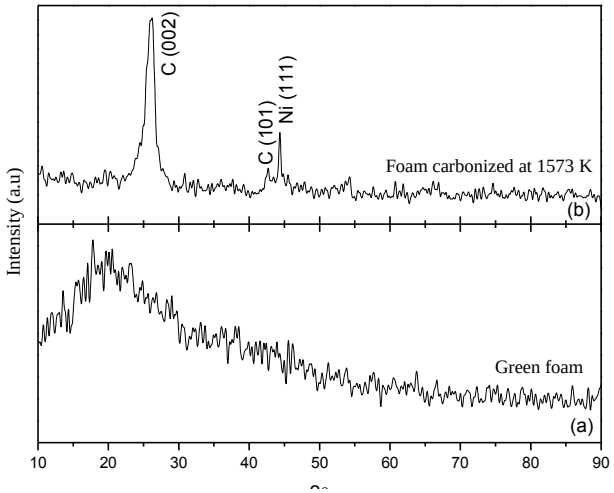

Fig. 8 XRD pattern of (a) NDCCAF (green foam) and (b) NDCCAF carbonized at 1573 K

DOI: 10.5963/AMSA0303005

Fig. 8 shows XRD pattern of green foam and NDCCAF carbonized at 1573 K. The XRD pattern of green foam shows a broad peak at 2θ value of 20.1 for carbon, which shifted to 26.2 on carbonization at 1573 K. The NDCCAF shows peaks corresponding to carbon (JCPDS file no. 89-8487) and nickel (JCPDS file no. 04-0850). XRD pattern of NDCCAF does not show any peak for alumina. This indicates that nickel and carbon are in the outer surface of the foam with alumina remaining as the inner structure. The density and porosity of NDCCAF are calculated and the values are 0.03 g. cm^{-3} and 99%, respectively.

Fig. 9(a) shows secondary electron microscopic image of NDCCAF. From the image, the average pore size was determined to be 260 μm. The foam exhibited pores of near spherical configuration that were interconnected by other pores and separated with solid struts with 50 μm thickness. To know nickel distribution over the foam surface, X-ray elemental mapping was carried out. Fig. 9(b) shows the X-ray mapping of nickel indicating uniform distribution of nickel over the foam surface (dimension of the foam 15 mm × 10 mm ×10 mm).

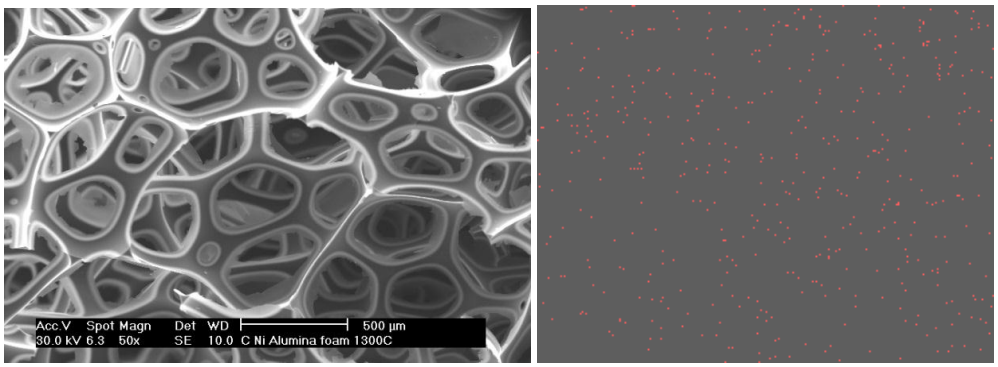

(a) (b)

Fig. 9 (a) Secondary electron microscopic image of NDCCAF and (b) X-ray mapping of nickel (colour dots) showing distribution on the surface of NDCCAF

C. CCNF

It is known that caramel is formed from aqueous solution of sucrose by heating at 373 K. Upon heating nickel foam with aqueous solution of sucrose at 383 K, the caramel formed was found to adhere to the surface of nickel foam. It was then heated to 1173 K in argon atmosphere. Like other carbohydrates, sucrose is decomposed at high temperatures to form CO_2 and H_2O in air leaving no residue. However, when heated in inert atmosphere, sucrose decomposes to form carbon. As the caramel coated nickel foam was heated to 1173 K in argon atmosphere, carbon coating was formed over the nickel foam surface. The density of CCNF was calculated to be 0.28 g. cm^{-3}, while the density of virgin nickel foam was found to be 0.22 g. cm^{-3}. The porosities of CCNF and virgin nickel foam were 97 and 97.5%, respectively.

Secondary electron microscopic image with the corresponding EDS spectra of CCNF is shown in Fig. 10 and is compared with that of virgin nickel foam as shown in Fig. 11. Fig. 10(b) shows an intense peak for carbon (Kα 0.277 keV) in addition to nickel indicating carbon deposition on nickel foam surface.

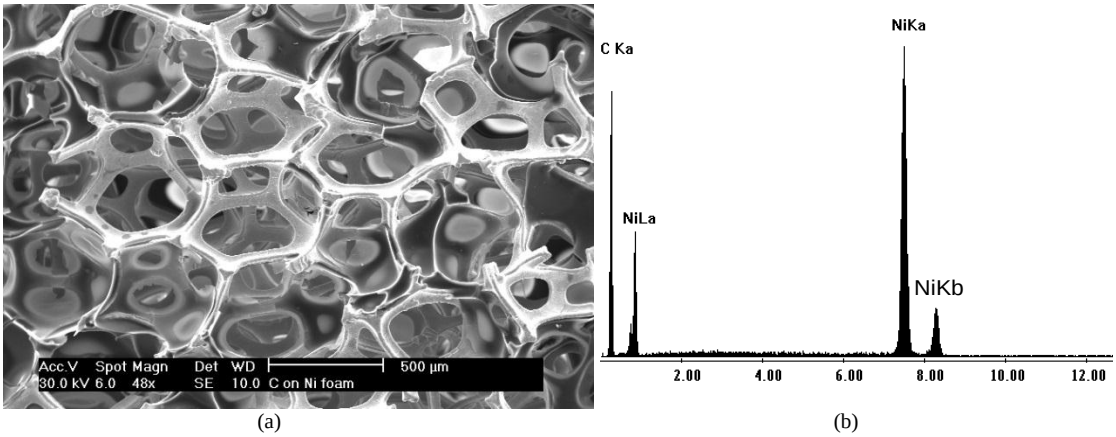

(a) (b)

Fig. 10 (a) Secondary electron microscopic image and (b) EDX spectrum of CCNF

DOI: 10.5963/AMSA0303005

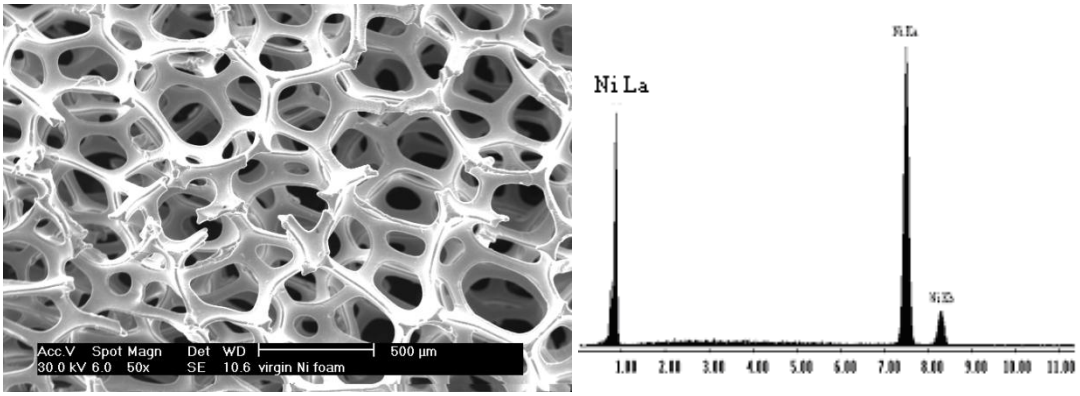

(a) (b)

Fig. 11 (a) Secondary electron microscopic image and (b) EDX spectrum of virgin nickel foam

Fig. 12 shows the pore at higher magnification of virgin nickel foam and CCNF. It was observed that pore and strut size/shape of CCNF were similar to that of virgin nickel foam and values were 200 and 50 μm, respectively, indicating morphological integrity after carbon coating. Grain size (10 μm) and shape of CCNF were also similar to that of virgin nickel foam as shown in Fig. 13 which is expected as the foam is formed by template method.

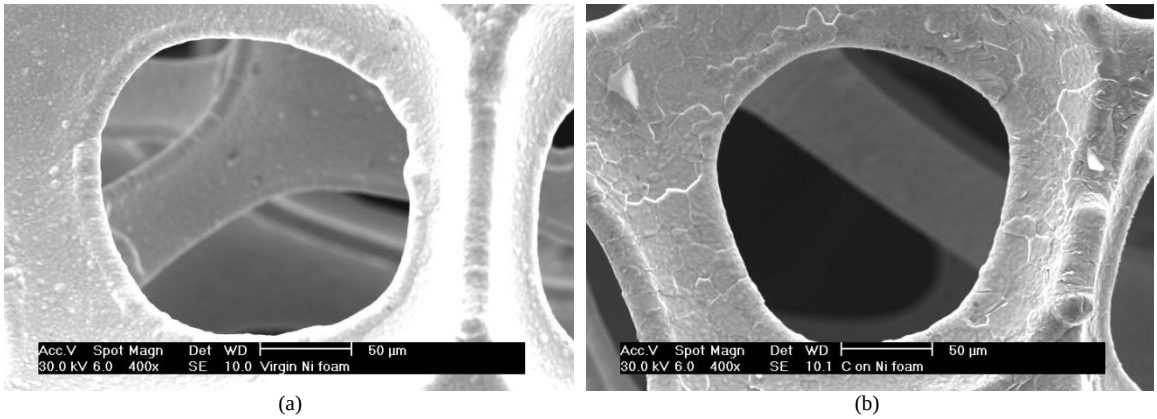

(a) (b)

Fig. 12 Secondary electron microscopic image showing pore size/shape of (a) virgin nickel foam and (b) CCNF

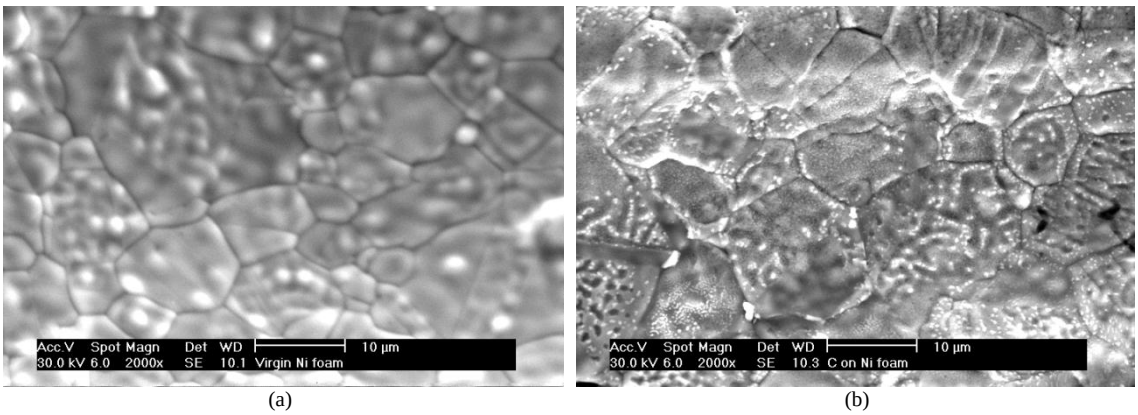

(a) (b)

Fig. 13 Secondary electron microscopic image showing grain size/shape of (a) virgin nickel foam and (b) CCNF

To analyze the carbon distribution over the surface of the foam, an X-ray elemental mapping of CCNF was carried out. Fig. 14 shows secondary electron microscopic image of CCNF along with X-ray elemental mapping of nickel and carbon. It was observed that carbon was coated uniformly over the nickel foam surface as shown in Fig. 14(c).

DOI: 10.5963/AMSA0303005

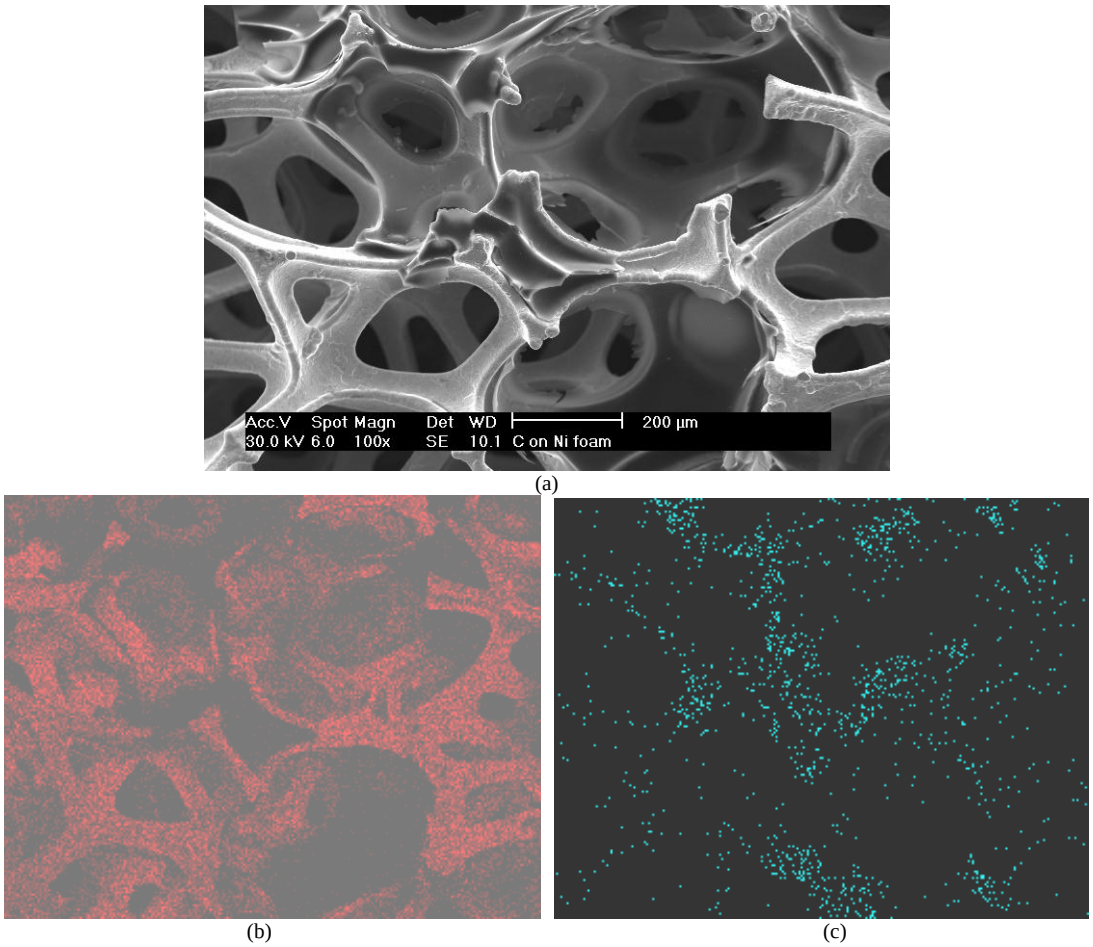

(a) (b) (c)

Fig. 14 (a) Secondary electron microscopic image of CCNF, X-ray elemental mapping of (b) nickel and (c) carbon (colour dots) in CCNF

Physical property of all the foams namely NDCF, NDCCAF and CCNF are summarized in the Table 1 below.

TABLE 1 PHYSICAL PROPERTY OF NDCF, NDCCAF AND CCNF

Samples	Density (g.cm^{-3})	Porosity (%)	Pore size (µm)
NDCF	0.09	96	200
NDCCAF	0.03	99	260
CCNF	0.28	97	200

IV. SUMMARY AND CONCLUSIONS

The NDCF was synthesized from aqueous solution of sucrose and $Ni(NO_3)_2$. Thermal analysis of green foam showed 73 wt% mass loss in five stages. The calculated bulk density of NDCF was 0.09 g. cm^{-3} and the porosity was 96%. The XRD pattern showed peaks corresponding to carbon and nickel. The average pore size was determined to be 200 µm for NDCF. X-ray elemental mapping indicates that nickel is uniformly distributed over the foam surface.

The NDCCAF with 0.03 g. cm^{-3} density and 99% porosity was synthesized from an aqueous solution of $Al(NO_3)_3$, $Ni(NO_3)_2$ and sucrose. Here, all the reagents are base materials and as well as pore formers. The thermo gravimetric study of the green foam showed 65% mass loss in five stages. The phase analysis by XRD revealed the presence of nickel and carbon in outer phase and alumina in the inner phase of NDCCAF. The surface morphology of NDCCAF, showed pores having near spherical shape held together by hexagonal edges with average pore size of 260 µm. X-ray elemental mapping indicates that nickel is uniformly distributed over the foam surface.

Unlike the other foam materials described above, CCNF was prepared through template technique by immersing nickel foam in aqueous solution of sucrose. Heating nickel foam with aqueous solution of sucrose at 383 K gives caramel coated nickel foam. The caramel coated nickel foam was carbonized to 1173 K in argon atmosphere. Therefore, carbon (residue of sucrose) was formed over the nickel foam surface. Porosity of CCNF was 97%. Pore and strut size/shape of the foam were unaltered indicating very thin coating of carbon on the struts of nickel foam. X-ray elemental mapping showed that carbon was uniformly coated on surface of the nickel foam.

DOI: 10.5963/AMSA0303005

Trapping efficiency of synthesized multi trap materials such as NDCF, NDCCAF and CCNF will be investigated very soon in liquid sodium (static as well as dynamic) to trap multi radionuclides such as ^{134}Cs, ^{137}Cs, ^{54}Mn, ^{58}Co, ^{60}Co etc.

ACKNOWLEDGMENTS

The authors acknowledge Mr. P. Muralidaran, Dr. R. Sudha, Mr. Sajal Ghosh, Dr. G. Panneerselvam and Mr. Raja Madhavan for their support. The authors also acknowledge Dr. K.S. Viswanathan for technical discussion and Dr. P. R. Vasudeva Rao for constant encouragement during the course of this work.

REFERENCES

[1] H. Feuerstein, A. J. Hooper, and F. A. Johnson, "Mechanism of release of radioactive products into liquid-metal coolants, their transport within the circuits and removal from LMFBRs," *Atomic Eng. Rev.*, vol. 17, pp. 697-761, 1979.

[2] Technical document on "Fission and corrosion product behavior in liquid metal fast breeder reactors (LMFBRs)," IAEA-TECDOC-687, pp. 9-155, 1993.

[3] V. Ganesan and P. Muralidaran, "Activity transport in fast reactor heat transport systems," Proceedings of the Nuclear and Radioachemistry Symposium (NUCAR-2007), Vadodara, India, pp. 69-76, 2007.

[4] W. H. Olson and W. E. Ruther, "Controlling cesium in the coolant of the experimental breeder reactor II," *Nuc. Tech.*, vol. 46, pp. 318-322, 1979.

[5] N. V. Krasnoyarov, V. I. Polyakov, A. M. Sobolev, and E. K. Yakshin, "The removal of cesium from the fast reactor primary sodium coolant," Proceedings of 3rd international conference on liquid metal engineering and technology (LIMET-1984), Oxford, vol. 3, pp. 185-189, 1984.

[6] K. Ch. Stade, H. H. Stamm, H. D. Hanke, and H. Clauss, "Status of cesium removal from primary sodium in the German LMFBR program," Proceedings of the international topical meeting on fast reactor safety, Knoxville, Tennessee, pp. 197-203, 1985.

[7] R. A. Bechtold and C. E. Grenard, "FFTF cesium trap design, installation and operating experience," Proceedings of 4th international conference on liquid metal engineering and technology (LIMET-1988), Avignon, France, ED SFEF F-75724, p. 609/1-10, 1988.

[8] N. Hanebeck, D. Msika, J. Misraki, R. Allegre, R. Tusche, and K. Ch. Stade, "Development of cesium traps for commercial sodium-cooled fast breeder reactors – ELCESNA, KNK II, RAPSODIE," Proceedings of 4th international conference on liquid metal engineering and technology (LIMET-1988), Avignon, France, ED SFEF F-75724, p. 631/1-14, 1988.

[9] T. Aoyama, T. Odo, S. Suzuki, and S. Yogo, "Operational experience and upgrading program of the experimental fast reactor JOYO," IAEA-TECDOC-1405, pp. 29-61, 2002.

[10] O. G. Romanenko, K. J. Allen, D. M. Wachs, H. P. Planchon, P. B. Wells, P. Nazarenko, I. Dumchev, V. Maev, B. Zemtzev, L. Tikhomirov, V. Yakovlev, and A. Synkov, "Cleaning cesium radionuclides from BN-350 primary sodium," *Nuc. Tech.*, vol. 150, pp. 79-99, 2005.

[11] Prasanta Jana and V. Ganesan, "Synthesis, characterization and radionuclide (^{137}Cs) trapping properties of a carbon foam," *Carbon*, vol. 47, pp. 3001-3009, 2009.

[12] J. C. McGuire and W. F. Brehm, "A radionuclide trap for liquid-metal-cooled reactors," *Nuc. Tech.*, vol. 48, pp. 101-109, 1980.

[13] Prasanta Jana, R.Sudha, A. Manivannan, Swapan Kumar Mahato, M. Lavanya, K. Chandran, P. Muralidaran, and V. Ganesan, "Studies related to development of radionuclide trap for removal of activated corrosion product ^{54}Mn from fast reactor," Proceedings of Nuclear and Radiochemistry Symposium (NUCAR-2011), Visakhapatnam, pp. 67-68, 2011.

[14] J. S. Brahmaji Rao, Prasanta Jana, E. Senthilvadivu, A. Manivannan, N. P. Seshadreesan, and P. Muralidaran, "Estimation of Mn using INAA and EDXRF in Ni foam, candidate radionuclide trap material for fast reactors," Proceedings of Nuclear and Radiochemistry Symposium (NUCAR-2011), Visakhapatnam, E-4, pp. 521-522, 2011.

[15] Prasanta Jana and V. Ganesan, "The production of a carbon-coated alumina foam," *Carbon*, vol. 49, pp. 3292-3298, 2011.

[16] Y. S. Han, J. B Li, and Y. J. Chem, "Fabrication of porous bimodal alumina ceramics," *Mater. Res. Bull.*, vol. 38, pp. 373-379, 2003.

[17] K. Prabhakaran, N. M. Gokhale, S. C. Sharma, and R. Lal, "A novel process for low-density alumina foams," *J. Am. Ceram. Soc.*, vol. 88, pp. 2600-2603, 2005.

[18] I. L. Finar, Organic Chemistry Vol I, "The fundamental principle," Six edition, ELBS, London, p. 503-530.

[19] B. V. L'vov, "Mechanism of carbothermal reduction of iron, cobalt, nickel and copper oxides," T*hermochem. Acta*., vol. 360, pp. 109-120, 2000.

DOI: 10.5963/AMSA0303005